

Josephson Effects in Superconductors

Advanced Lab Course

Experiment #16

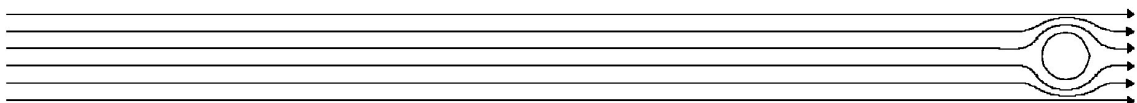
at the

Walther–Meißner–Institut

Physik-Department

Technische Universität München

March 27, 2017



Contents

1	Safety	4
1.1	Handling of liquid helium	4
1.2	Electronic measurement equipment	5
1.3	Food and drinks	6
2	Introduction	7
2.1	Superconductivity	7
2.2	Josephson effects	11
2.2.1	Theory	11
2.2.2	Josephson equations	12
2.2.3	Josephson contacts	13
2.2.4	DC - Josephson effect	14
2.2.5	AC - Josephson effect	14
2.2.6	Josephson contacts in the magnetic field	14
2.3	I-U Characteristics of Josephson Junctions	16
2.4	Radiation emission	17
2.5	Point Contacts	17
2.6	Layer Contacts	18
2.7	Summary of fundamental terms	18
3	Experimental Setup	20
3.1	Sample	20
3.2	Sample Holder	20
3.3	Measurement Equipment	22
4	Measurement	26
4.1	Cooling down the sample rod	26
4.2	Measuring the I-U-curve	26
4.3	Measurement of the field dependent critical current	27
4.4	Warming up the sample rod	28

5	Exercises	29
5.1	Questions	29
5.2	Evaluation	29
5.2.1	Introduction	29
5.2.2	Zero field measurement	30
5.2.3	Field dependent measurements	30

Chapter 1

Safety

This experiments includes operating a low-temperature cryostat and the handling of cryogenic liquids, in particular liquid helium. The latter has a boiling point of 4.2 K and thus, when exposed to skin, can cause severe cold burn and frost bite. Furthermore, if larger quantities of liquid helium are spilled, the gaseous helium can replace the oxygen in the laboratory and cause hereby asphyxiation.

The tutor will give a safety briefing covering a risk assessment of the experiments and the proper use of the safety equipment. Handling of the equipment is only permitted in attendance of or after consulting the tutor!

1.1 Handling of liquid helium

General

At the Walther-Meißner-Institut liquid helium is operated in a closed cycle system. Helium dewars – the storage and transport vessels for liquid helium – must be connected to the return line as otherwise pressure will build up in the vessel. Nevertheless, dewars are designed to provide means of transportation for liquid cryogens and therefore transport within the building is permitted. Tilting and tipping the dewar has to be prevented at all times, as in this case the liquid helium gets in contact with "hot" parts of the dewar resulting in a quick pressure build-up and emergency gas relief. The transport of liquid cryogens in the elevator is permitted only without accompanying persons.

Dangers

The work with liquid helium and equipment in touch with cryogens requires special safety measurements. When operating equipment which is or was cooled by liquid or gaseous (cold) helium or removing equipment from cryostats/dewars, please keep in mind that this equipment is cold. In particular, direct skin contact will cause severe cold burns and frost bites requiring medical treatment. The same holds true for the

exposure of skin to cold gas or the cryogenic liquid itself. There's also the danger of asphyxiation if large quantities of liquid/gas are relieved from the dewar or cryostat (lack of oxygen). In the case of uncontrolled escape of helium the room has to be evacuated immediately.

Safety measures

- Always wear personal protective gear while working with the helium dewar, i.e. special (blue) cryogen gloves and safety goggles.
- Keep the door to the lab open to ensure oxygen flow in the room.
- Check that the helium dewar is positioned upright on an even surface.
- Ensure that the helium is connected to the return line. Exceptions are during helium transfer and transport of the dewar.
- When you insert or remove the dipstick into the dewar ensure to do so in a controlled and slow manner. For this please check the optimum adjustment of the clamp. Dangers: Abrupt lowering may lead to a quick evaporation of large quantities of helium and thus might result in an emergency gas relief (danger of asphyxiation). This could lead to breakdown of the insulation vacuum (resulting in even larger quantities of gas).

1.2 Electronic measurement equipment

For your measurements you will use electronic equipment which is powered through the 230 V mains. I.e. inside all electronics 230 V are present. Thus all electronic appliances must be kept closed and no covers/chassis may be removed at any time. Additionally, the device and electronics used for your experiment are highly sensitive and thus laying out the measurement circuit and setting it up must be discussed with the tutor. Reconnecting/changing the wiring of the setup must be consulted and approved by the tutor – she/he must be present in the lab for this task.

Dangers

Physical contact with the mains supply of 230 V may be lethal! Therefore, any modifications to the equipment is forbidden. You must not open any pieces of equipment. Modifications to the setup are only to be done by the tutor. The assembly of the signal lines can be changed without danger.

Any problems with the equipment have to be reported to the tutor immediately.

Further information concerning safety can be found in the "red folder" in the laboratory.

1.3 Food and drinks

It is not allowed to consume food and beverages in the lab. If you need a break and want to eat or drink something, please do so outside of the lab. Please, be reminded about your personal hygiene, such as washing your hands prior to consuming foods and drinks. If you want to take a longer break, please tell the tutor.

Chapter 2

Introduction

2.1 Superconductivity

Superconductivity is a thermodynamic state of the solid state which is entered when the body is cooled below a critical temperature T_c . The two most prominent features of the superconducting phase are the repelling of magnetic fields out of the body and the existence of a zero-resistance state. The latter was first discovered by Heike Kamerlingh Onnes in 1911 at Leiden when the metal mercury revealed a state of infinite conductivity below the temperature of liquid helium [1]. Figure 2.1 shows the resistance values of mercury as function of temperature around the critical temperature T_c . This resistance behavior was entirely unexpected at that time as it was thought that the conductivity of metals will vanish at low temperatures. The argument was that the kinetic energy of the electrons will tend towards zero for zero temperatures. Thus, it was expected that the metal will enter a high resistance or insulation state. Exactly the opposite result was observed: the conductivity increased during the cooling process and suddenly jumped to infinity at 4.2 K corresponding to vanishing or zero electrical resistivity. It took two more decades to theoretically explain this phenomenon on a microscopic level [3, 4].

Electrical conductivity in a solid is mediated by charge carriers, usually electrons. In an ordered crystal charge carrier motion is described with the Bloch model. In this quantum mechanical model electrons are described as wavefunctions. Up to this point the resistance is not included in this model. This changes, when scattering centers such as crystal imperfections or defects, lattice distortions called vibrations or phonons, or higher order effects such as electron-electron interaction comes into play. Nevertheless, superconductivity is incompatible with this description as the phenomenon was also experimentally observed in disordered and imperfect solids at finite temperatures.

The superconducting state is a property of the electron system, where the electrons are able to move non-dissipatively, similar to electrons in atomic orbitals or molecules. Furthermore, spectrally resolved absorption experiments in the far infrared regime indicate that superconductors have an energy gap. Additionally, long range order in the

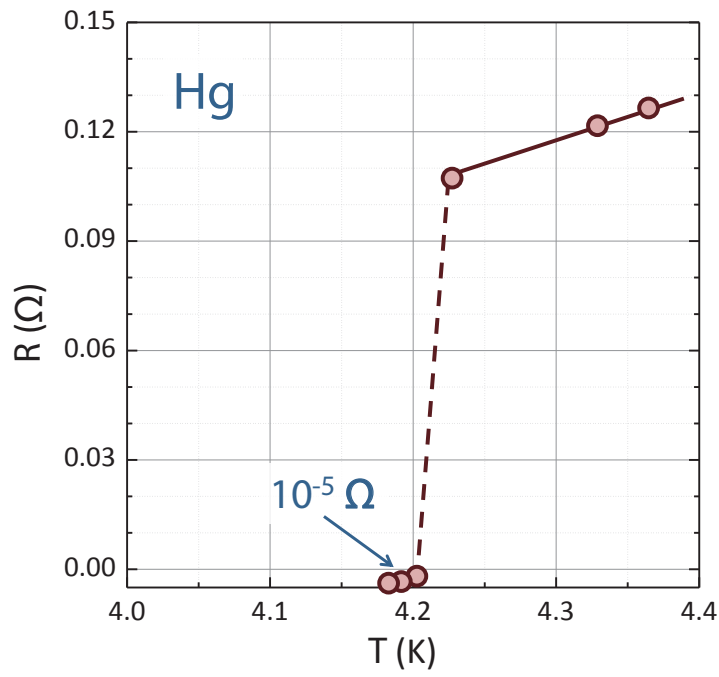


Figure 2.1: Superconductivity in mercury. Below $T = 4.2$ K the mercury has a vanishing resistance. The data shown is taken from the original publication of Onnes (cf. Ref. [1]). The data graph is taken from [2].

conduction electron system is observed. A complete explanation for these observations started with the suggestion by Fröhlich that an attractive interaction between the electrons mediated by phonons might give rise to a superconducting state. This idea was taken up by Cooper [5–7] and eventually lead to the formulation for the BCS theory for superconductivity [3, 4]. The key idea is that electrons form pairs in the phase space, so-called Cooper pairs. The momentum state of these pairs can be thought of two electrons with opposing momenta and spin states $|\mathbf{p}_i \uparrow, -\mathbf{p}_i \downarrow\rangle$. If one of the electrons is scattered that second one can compensate for this scattering event. Thus, when exposed to an external force, e.g. an electric field, $|(\mathbf{p}_i + \mathbf{P}/2) \uparrow, (-\mathbf{p}_i + \mathbf{P}/2) \downarrow\rangle$, where \mathbf{P} is the momentum of the cooper pair. Here, in \mathbf{P} , contrary to the single electron case, no momentum distribution is present. Thus, the entire ensemble of Cooper pairs moves with momentum \mathbf{P} allowing to summarize the behavior of these quasi particles with a macroscopic wavefunction

$$\Psi_P = \Psi \exp(i\phi(r)) \quad (2.1)$$

with $\phi(r) = \mathbf{P} \cdot \mathbf{r}/\hbar$. Therefore, the whole superconductor appears to the electrons as a (giant) molecule in which the wave packets move with a stable phase relation. In a current-free state, this phase is a constant in space. If the phase varies with space ($\frac{\partial}{\partial x}\Psi(r_i) \neq 0$), a super-current appears.

One consequence of the macroscopic wavefunction are quantized boundary conditions for ring like structures, i.e. the wavefunction must interfere constructively like in Bohr's model of the atom. This condition is called the fluxoid quantization condition.

More fascinating effects can be observed, when two superconductors are brought into weak contact with each other - via a geometrically thin contact (e.g. a tip contact), an oxide layer or a conducting (but non-superconducting) layer. The principle of such contacts is shown in Fig. 2.3

While the phase of the center of mass of the superconducting electrons in the superconductors SC 1 and SC 2 are well defined, it is now possible - due to the weak coupling - to have a phase shift between SC 1 and SC 2. In the theory of superconductivity by Bardeen, Cooper and Schrieffer (BCS-theory, 1957) [3, 4], the electrons in the superconducting electron gas are correlated in pairs (Cooper pairs) whose binding energy (despite the low entropy) stabilizes the superconducting state with regard to the normal (non-superconducting) state. A Cooper pair can be basically regarded as wave packed with the extension of the coherence length ξ ($\xi \approx 10^4 \text{ \AA}$). For contact layers between both superconductors considerably thinner ($\approx 10 - 10^2 \text{ \AA}$), it is possible that Cooper pairs are able to tunnel between both superconductors without being destroyed, which is similar to the possibility of weak supercurrents (Josephson current) between SC 1 and SC 2. Josephson effects contain the correlation of the Josephson currents between SC 1 and SC 2 as well with and without magnetic field (in the contact layer) as with and without difference in the electrical potential between SC 1 and SC 2.

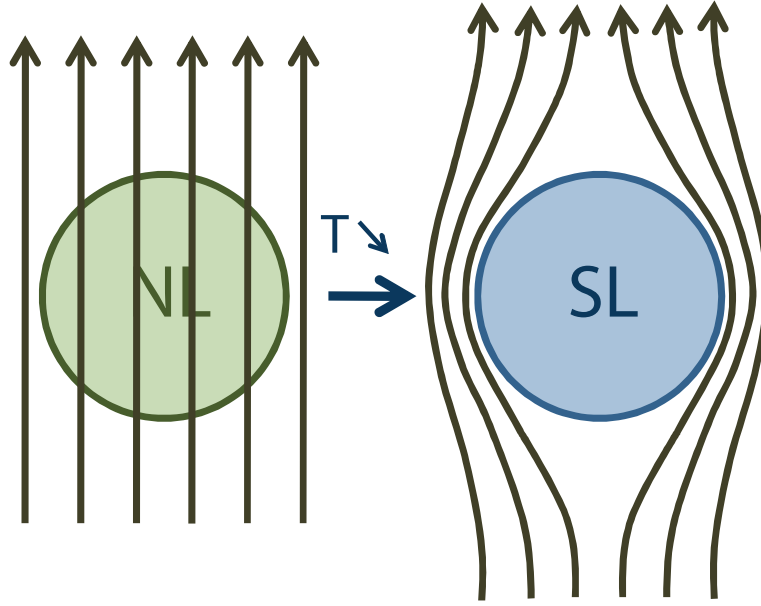


Figure 2.2: A sketch of the Meißner effect. An external magnetic field penetrates the material when $T > T_c$ (left side), but is expelled when the temperature is lowered below the critical temperature T_c (right side). Picture taken from [2].

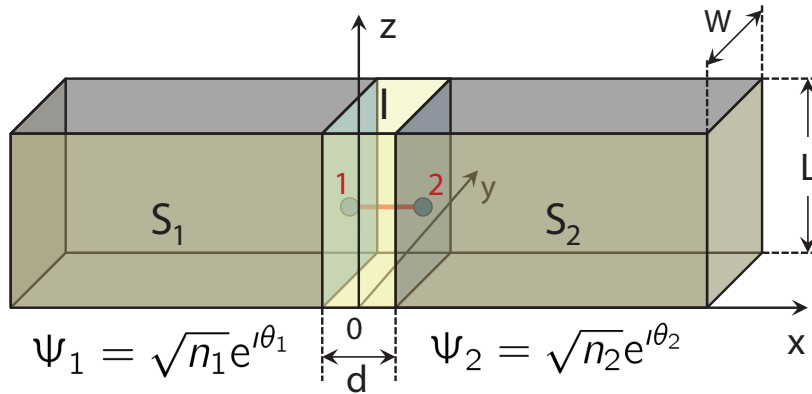


Figure 2.3: Sketch of a Josephson junction, consisting of two superconducting layers (S_1 and S_2) and an isolating layer I . Picture taken from [2].

2.2 Josephson effects

Some of the most important applications of superconductivity are connected with Josephson effects, e.g. extremely fast switches. Another application is the measurement of magnetic flux (to the precision of a fraction of a flux quantum) with two Josephson contacts (also called Josephson junctions) embedded into a ring structure.

The task of this experiment is to examine a niobium layer contact. The experimental setup allows to survey I-U characteristics of the Josephson junction and allows measurements of the critical current of the junction as a function of flux through the junction.

2.2.1 Theory

Superconductivity is a quantum phenomena on macroscopic scale. The BCS theory describes the superconducting state as a condensate of electrons bound in pairs (Cooper pairs), which are correlated with fixed phase. The total wave function can be written as

$$\Psi = \sqrt{n_S} \cdot \exp(i\varphi(\vec{r})) \quad (2.2)$$

with the density of Cooper pairs n_S and the phase of the wavefunction φ . Ψ can be taken as the movement of the center of mass of the superconducting electrons. The general expression for the quantum mechanical current is

$$\vec{j} = \frac{iq\hbar}{2m^*} \cdot (\Psi \vec{\nabla} \Psi^* - \Psi^* \vec{\nabla} \Psi) - \frac{q^2}{m^*c} \cdot \vec{A} \cdot \Psi \Psi^*. \quad (2.3)$$

With the space independent density of Cooper pairs n , $q = -2e$ and $m^* = 2m$, we derive

$$\vec{j} = -\frac{\hbar en}{m} \cdot \vec{\nabla} \varphi - \frac{2e^2 n}{mc} \cdot \vec{A} \quad (2.4)$$

with the elementary charge e and the electron charge m . Eq. (2.4) shows the relation between the current density \vec{j} in the superconductor, the phase of the wavefunction φ and the vector potential \vec{A} . From eq. (2.4) the 2. London equation can be derived $\vec{\nabla} \times \vec{j} = -\frac{1}{\lambda_L^2} \vec{B}$ [8, 9], which leads to the understanding of the Meißner effect [10].

As the current density has to be gauge invariant, it can be deduced that for the gauge transformation $\vec{A} \rightarrow \vec{A} + \vec{\nabla} \chi$ the phase of the wavefunction transforms into

$$\varphi \rightarrow \varphi - \frac{2e}{\hbar c} \chi \quad (2.5)$$

which is equivalent to gauge invariance - as the equation is independent of the choice of the vector potential \vec{A} , to which a gradient of an arbitrary potential function χ can be added without altering the magnetic field \vec{H} :

$$\begin{aligned}\vec{A}' &= \vec{A} + \nabla\chi \\ \vec{H} = \text{rot}\vec{A}' &= \text{rot}\vec{A} + \underbrace{\text{rot}\nabla\chi}_{\equiv 0} = \text{rot}\vec{A}\end{aligned}\tag{2.6}$$

2.2.2 Josephson equations

For two superconductors linked via a weak link (a region with obviously reduced contribution of the order parameter Ψ) - see fig. 2.3 - the whole system is still described by a uniform condensate wavefunction. Unpaired electrons as well as Cooper pairs are able to cross the region of the weak link - the resulting effects were predicted by B.D. Josephson in 1962.

The current over a barrier between two superconductors depends on the phase difference $\gamma = \varphi_2 - \varphi_1$ between both sides $j_{12} = f(\gamma)$, which is analog to the correlation between current and phase gradient within a superconductor (eq. 2.4).

As a time reversal transformation changes the direction of the current and the sign of the phase, this implies that the current needs to be an odd, 2π periodic function of the phase difference γ . It can be shown that - under the assumption of a weak coupling (e.g. tunnel contact) - the first fourier component of the evolution of f to the phase difference is sufficient, which means that j_{12} is a sine of the phase difference:

$$I = I_c \sin \gamma\tag{2.7}$$

This equation is known as first Josephson equation. The critical current I_c at $T = 0$ for a tunnel contact is proportional to the energy gap: $I_c \propto \Delta$ (Ambegaokar-Baratoff-relation).

Since the Josephson current has to be gauge invariant as well, in the presence of a magnetic field the corresponding term of the vector potential in the gauge invariant phase difference has to be considered:

$$\gamma = \varphi_2 - \varphi_1 + \frac{2e}{\hbar c} \int_1^2 \vec{A} \cdot d\vec{s}\tag{2.8}$$

If the current is increased over the value of the critical current I_c of the weak link, the current cannot be carried by the supercurrent alone. The resistivity R_n of the additional, normal conducting electrons leads to a potential difference and therefore to a voltage U between the two still superconducting regions. To describe this state quantitatively, the effect of a gauge transformation on the properties of a time-independent scalar electro-magnetic potential Φ has to be taken into account:

$$\Phi \rightarrow \Phi - \frac{1}{c} \frac{\partial \chi}{\partial t}\tag{2.9}$$

This equation together with eq. 2.5 leads to the gauge invariant 2. Josephson equation

$$\dot{\gamma} - \frac{2e}{\hbar} \cdot U = 0 \quad (2.10)$$

We conclude:

- the first Josephson equation correlates the phase difference at the Josephson contact with the current of the Cooper pairs over this contact
- the second Josephson equation shows that the phase difference γ changes linearly with time in case of a potential difference between both superconductors

2.2.3 Josephson contacts

Josephson effects can be studied on various different contact types beside the tunnel contact discussed above: e.g. on point contacts (fig. 2.4 (e)) via a tip or layer contacts (fig. 2.4 (a,b)), which are studied in this experiment.

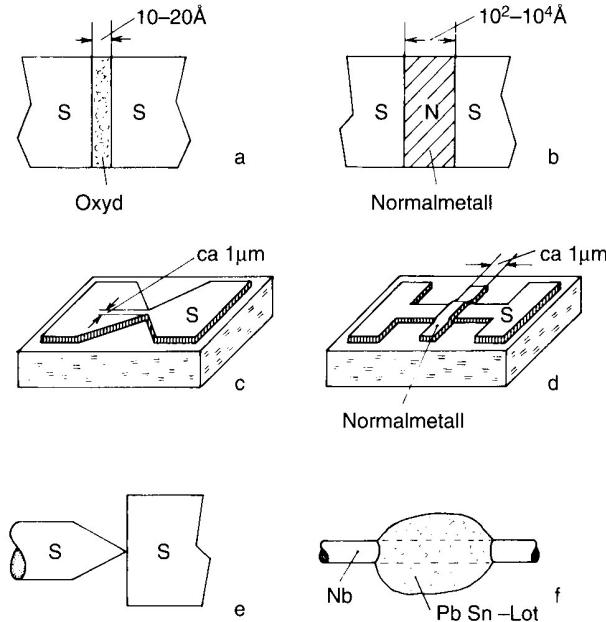


Figure 2.4: Common types of Josephson contacts (see [11]) a) Oxide layer; b) SNS–contact; c) film contact; d) Double layer contact via Proximityeffects; e) point contact; f) multiple point contacts (SLUG).

2.2.4 DC - Josephson effect

For a contact without a potential difference between both superconductors, we derive from eq. 2.10: $\gamma = \gamma_0 = \text{const.}$ Therefore a current constant in time over the contact is derived from eq. 2.7: $I = I_c \cdot \sin \gamma$, which lies within the range given by $\pm I_c$ (critical current).

This equation is similar to the equation of coupled pendulums: no energy is exchanged if the pendulums are oscillating in phase or out of phase. The maximal energy exchange takes place for a phase shift of $\pm\pi/2$.

2.2.5 AC - Josephson effect

In case of a temporally constant voltage U between both superconductors, we derive from eq. (2.10): $\gamma = \gamma_0 + (2e/\hbar)Ut$ and from eq. (2.7)

$$I = I_c \cdot \sin(\gamma_0 + \frac{2e}{\hbar}Ut) \quad (2.11)$$

follows that an AC current with the frequency

$$f = \frac{2e}{h} \cdot U \quad (2.12)$$

is flowing over the contact. As $2e/h = 483.6 \text{ MHz}/\mu\text{V}$, this frequency lies in most cases in the microwave regime for experimentally exploitable voltages. The emitted radiation (frequency f) can be measured radiometrically.

A second explanation is possible for the AC Josephson effect: the tunneling Cooper pairs are accelerated due to the presence of the voltage U and gain the energy $2eU$. As the Cooper pairs are not allowed to alter their energy while tunneling, a photon of the energy $hf = 2eU$ (eq. (2.12)) is emitted.

2.2.6 Josephson contacts in the magnetic field

Taking the finite size of the Josephson contacts into account, a correlation between I and the magnetic flux Φ through the contact is derived from eq.(2.8). It can be shown that this correlation has the form:

$$I_c(H) = I_c(0) \cdot \left| \frac{\sin\left(\frac{\pi\Phi}{\Phi_0}\right)}{\frac{\pi\Phi}{\Phi_0}} \right| \quad (2.13)$$

with $\Phi = (2\lambda_L + d) \cdot L \cdot B$ (see e.g. Ref. [11]), the thickness of the non-superconducting layer d , the size of the contact perpendicular to the magnetic field L and the London penetration depth λ_L . This function is plotted in graph 2.5. Note that the form is equivalent to that of bending on a slit.

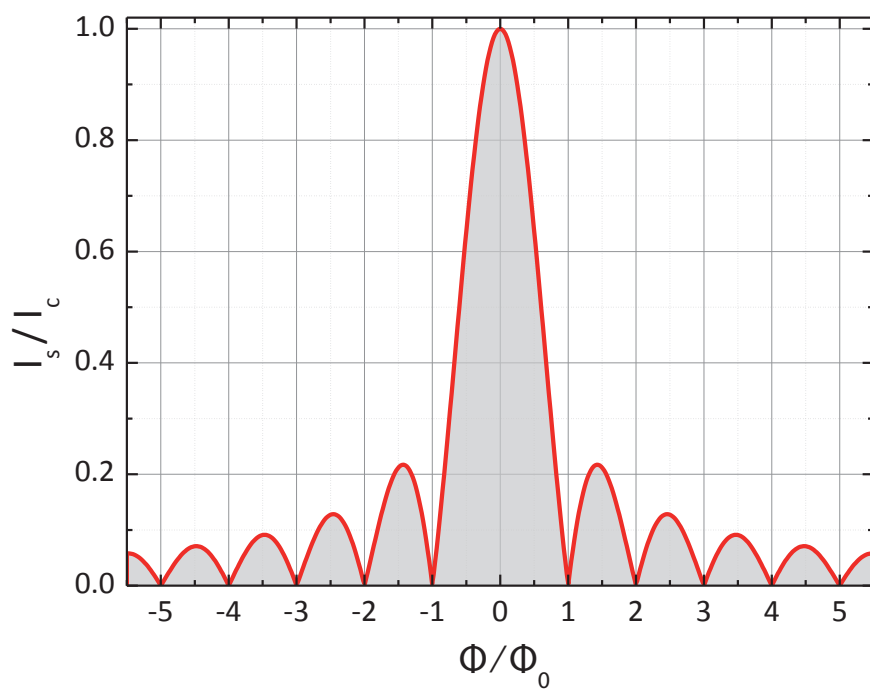


Figure 2.5: Dependence of the critical current I_s (or $I_c(H)$) of a Josephson contact on the magnetic field, divided by the critical current at zero external field I_c (or $I_c(0)$). Picture taken from [2].

2.3 I-U Characteristics of Josephson Junctions

The normal conducting electrons and the capacitance between the electrodes also affect the $I - U$ characteristics of a Josephson junction. Those two contributions are taken into account by the RSJ-model (Resistively Shunted Junction). The equivalent circuit is shown in fig. 2.6.

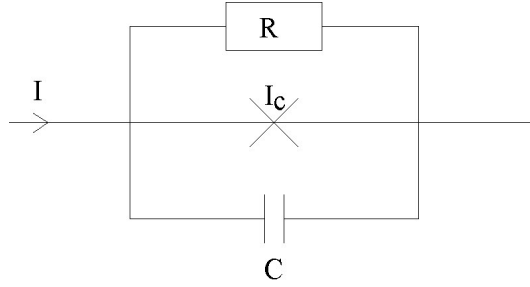


Figure 2.6: Equivalent circuit of a Josephson junction according to the RSJ-model.

The total current across the junction is given by

$$I_{tot} = I_c \cdot \sin \gamma + \frac{U}{R_n} + C\dot{U}. \quad (2.14)$$

In order to record such an $I - U$ characteristic, the Josephson junction is biased with a current I_{tot} and the voltage drop across the junction is measured. Due to the nonlinear behavior, the frequency spectrum of the current does not contain only the basic frequency according to equation (2.12) but also higher harmonics.

Inserting the second Josephson equation (2.10) in equation (2.14) yields a non-linear differential equation for γ that corresponds to that of a physical pendulum [12]. Solving this differential equation numerically, one has to distinguish two limits with respect to the so called McCumber-parameter β_c

$$\beta_c := \frac{2\pi C R_n^2 I_c}{\Phi_0} \quad (2.15)$$

(β_c is a measure of the Q factor of the resonant circuit, $\Phi_0 = h/2e$ is the flux quantum.)

- $\beta_c > 1$ (underdamped)

For $I < I_c$ there are two stable solutions. Therefore, the $I - U$ curve becomes hysteretic (fig. 2.7a). Starting at zero current and increasing the bias current does not produce any voltage drop across the junction until the critical value I_c is reached. At I_c the voltage is switched from zero to a finite value within $1ps$. This rapid switching behavior is used in Josephson devices. If I is now reduced below I_c , U does not drop back to zero until a retrapping current I_R is reached.

This hysteresis can be used to estimate the McCumber-parameter β_c :

$$\frac{I_R}{I_c} = \frac{4}{\pi\sqrt{\beta_c}} \quad (2.16)$$

- $\beta_c < 1$ (overdamped)

The $I-U$ curve shows no hysteresis (fig. 2.7b). In the limit of vanishing capacity $\beta_c = 0$ and the differential equation can be solved analytically. The time averaged voltage drop $\langle U(t) \rangle$ is for $|I_{tot}| > |I_c|$

$$\langle U(t) \rangle = \pm R_n \sqrt{I_{tot}^2 - I_c^2} \quad (2.17)$$

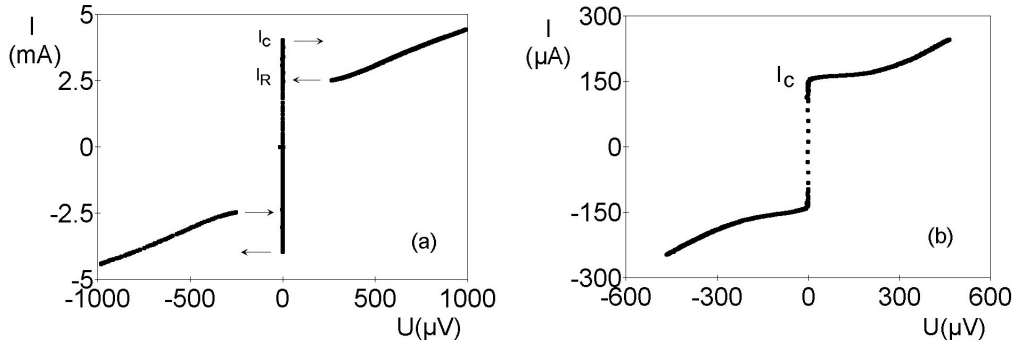


Figure 2.7: Typical current-voltage-curve (a) of a tunnel junction, (b) of a weak link.

2.4 Radiation emission

The radiating power at a frequency ν depends on several parameters of the Josephson junction. Due to the nonlinearity of the Josephson junction a part of the radiating power is used for the emission of higher harmonics. Furthermore the radiated power is determined by the impedance matching of the Josephson junction to the characteristic impedance of the space. Fig. 2.8 shows an emission curve measured as a function of voltage on a point contact.

2.5 Point Contacts

A superconducting point contact consists of two superconductors, coupled by a very small area. Experimentally, this is realized by pressing a superconducting tip to a flat superconducting surface. Naturally, this experimental setup is not well defined, for the properties of this contact depend among other things on the physical pressure

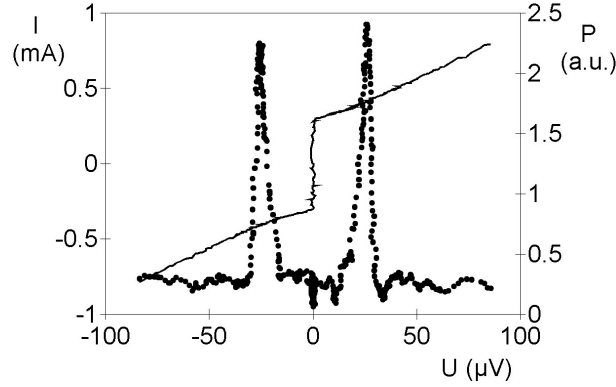


Figure 2.8: Characteristic of a Nb-Contact (straight line) and radiometersignal P at $f = 12.75$ GHz (points).

and the oxidation at the surfaces of the superconductors. Nevertheless there are two limiting cases that can be distinguished. Under very small pressure the junction can be dominated by the oxide layers and therefore show tunneling behavior. On the other hand under high pressure, a small metallic contact between the two superconductors can result in a weak link behavior. With the experimental setup described above, both $I - U$ characteristics in fig. 2.7 were measured. Varying the pressure between the superconducting tip and the superconducting surface between these limits yields other $I - U$ -characteristics that probably result from a parallel connection of metallic paths and tunneling contacts.

Due to the often varying properties of the point contacts in this experimental setup they show a bad reproducibility.

2.6 Layer Contacts

Due to its fixed nature, layer contacts offer a much better reproducibility than e.g. point contacts. Layer contacts consist of two superconducting layers which are separated by a non-superconductor. Popular layer contacts are e.g. Nb/Al_x/Nb contacts which are also used in this experiment. The contact is created in a multilayer process, where the different layers are placed on the substrate one after another. The structure of each layer is defined by optical lithography.

Depending on the geometry/size of the structure both overdamped and underdamped junctions can be built.

2.7 Summary of fundamental terms

You should know the meaning of the following terms:

-
- critical temperature T_c
 - Cooper pair
 - Meißner effect, ideal diamagnetism
 - London penetration depths
 - Flux quantum
 - Josephson contact, tunnel current
 - Josephson equations
 - DC- and AC-Josephson effect
 - Current-Voltage characteristics of Josephson contacts
 - McCumber-parameter and damping of Josephson junctions

Chapter 3

Experimental Setup

3.1 Sample

You will examine a thin film layer contact consisting of niobium as superconductor and aluminium oxide (AlO_x) as the separating layer. The niobium layer is 100 nm thin, the thickness d of the AlO_x is 17.83 nm. The thin films are placed on a $6\text{ mm} \times 10\text{ mm}$ silicon substrate which is $250\text{ }\mu\text{m}$ thick. The junction area is a square with an edge length L of $19.5\text{ }\mu\text{m}$.

3.2 Sample Holder

The sample is located inside a brass box. The box is fixed at the bottom of a so called dip stick (see fig. 3.1), which can be inserted into a liquid helium can to cool down the sample. This is an easy and fast way to reach a temperature of the sample of 4.2 K, which is sufficient for the experiment as the critical temperature T_c for niobium is 9.2 K.

Inside the box, the sample is mounted on a board, which is used to connect the junction to the wiring of the dip stick, to allow for a connection to the measurement equipment. For this, the contact pads of the junction are connected to large copper pads on the board using bonds (thin aluminium wires). In addition, pin connectors are soldered to these copper pads, which are used to quickly connect the dip stick wiring to the chip.

The sample resides in the bore of a small coil, which can be used to create a magnetic field, oriented parallel to the substrate surface and normal to the non-superconducting interface.

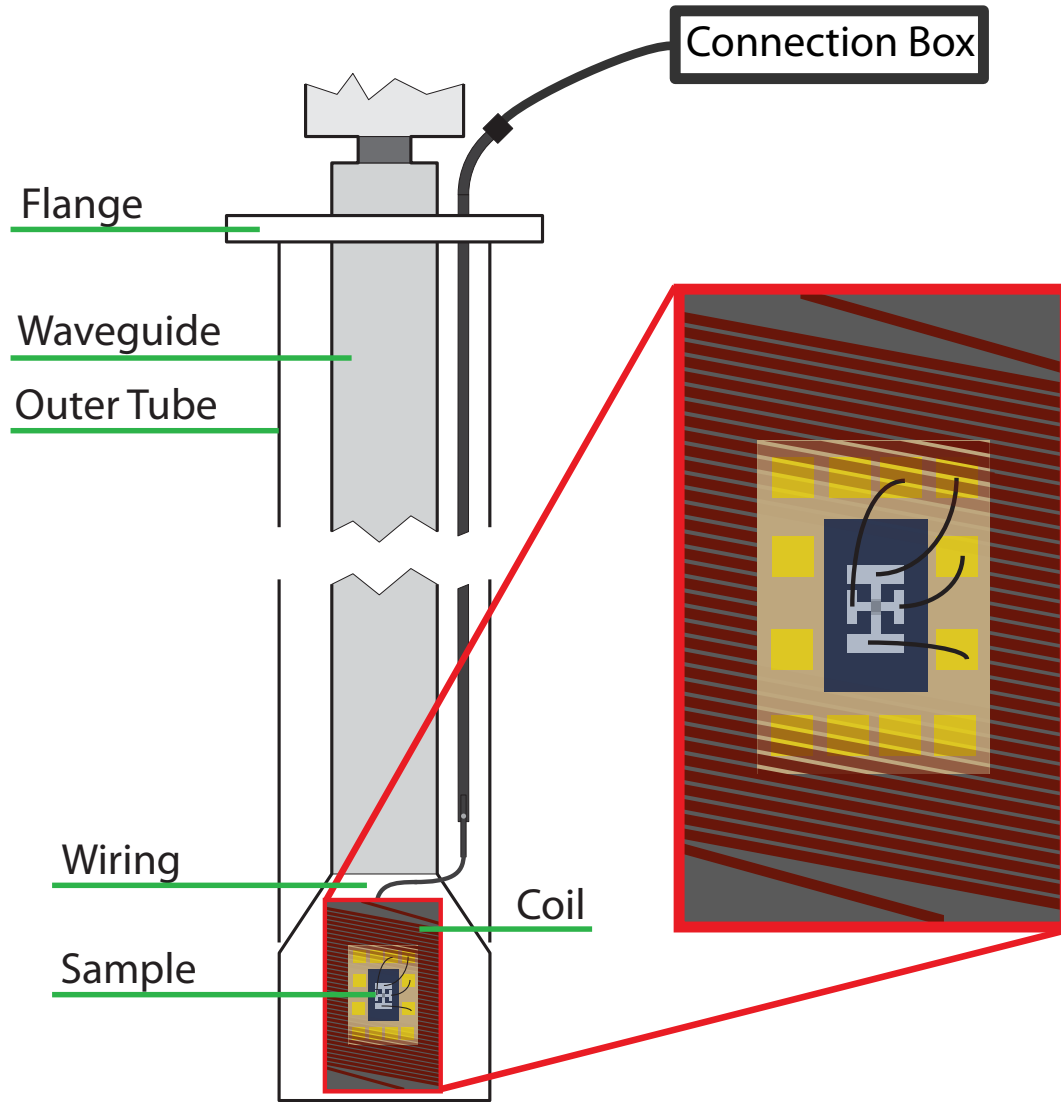


Figure 3.1: Sketch of the sample rod. The sample with the Josephson contact (grey and blue) is located inside a coil (copper-colored), which is fixed at the bottom of the dipstick. The junction is mounted on a board (light brown) and connected to pads on the board (yellow) with aluminium bonds (black). The board itself is connected to the connection box of the NIM-frame (see Sec. 3.3) with wiring placed inside the dipstick.

3.3 Measurement Equipment

The measurement equipment is placed in a NIM-frame (Nuclear Instrumentation Module) as it is shown in Fig. 3.2).

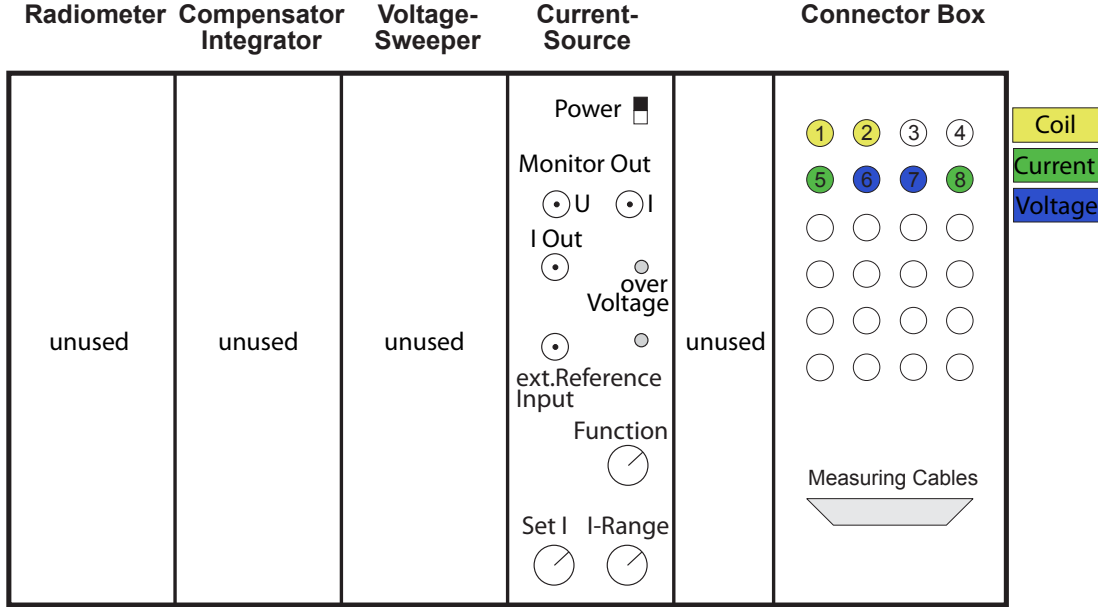


Figure 3.2: Drawers of the NIM-frame. In use for this experiment are the current source for the magnetic coil and the connector box. I Out of the current source is connected to ports 1 and 2 at the connector box (yellow), the current applied to the junction is connected to ports 5 and 8 (green) and the voltage measurement is connected to ports 6 and 7 (blue).

Measurement setup for Current and Voltage

In the experiment we use a digital source measure unit (SMU) to measure the I-U characteristic of the Josephson contact. The instrument can be used to drive a current between two output ports and simultaneously measure the voltage drop between an additional set of two ports. With this, and the right wiring at the sample, we are able to perform a four point (also called four wire) measurement, which allows us to neglect the resistance of the long in- and output wires.

The cables used to drive the current are connected to the two "force hi" ports of the SMU and on the other end to ports 5 and 8 at the connector box (see fig. 3.2, green ports). The cables used for the voltage measurement are connected to the "sense hi" ports of the SMU and to ports 6 and 7 at the connector box (blue ports).

The SMU is connected to a measurement computer with a standard LAN cable. With this, the measurement and all the important settings can be controlled with a LabView measurement program.

Measurement setup for field dependent measurements

The current source in figure 3.2 is used to drive a current to the coil in order to control the magnetic field inside the junction. The current can be set to $\pm I_{\max}$, where the maximal current I_{\max} can be varied between 1 μA and 100 mA by turning the knob I-Range. This current is available at **I-Out**, that has to be connected to the coil (connectors 1 and 2). In addition to that, the current source supplies a monitor voltage signal at **Monitor Out - I**. The monitor signal is directly proportional to the current and in each current range, the maximal current corresponds to a monitor signal of 1 V. It is connected to a voltmeter, that is used to view the applied coil current.

LabView Program

The SMU used for the measurement can be completely controlled by a LabView program. Figure 3.3 shows a screen shot of the program. This section will explain all the settings you can change with the program and how to perform and save a measurement.

On the far left side you can find the basic settings. At the top is a setting for the **Visa resource name**, which sets the TCPIP address of the measurement device. Going from top to bottom, **Source Mode** sets whether you want to drive a current or a apply voltage to the system. **Limit Level** is the maximal measured value, which means, if **Source Mode** is set to current and the measured voltage exceeds the **Limit Level**, the measurement program will stop. **Delay** sets the delay between each measurement point. **Measurement Speed** sets the number of power line cycles, that the instrument takes to perform a measurement. These first five settings should be set to the values seen in the screenshot and should not be changed during the experiment. The three settings in the **Define Sweep** part set the **Start** and **Stop** value of the measurement (in A or V) and the **Number of Points** which are recorded. Next to the **Source Mode** setting you can change the sweep mode (**Enable Up-Down Sweep**). If the light is on, the current is ramped up to the set **stop** value and afterwards ramped back down to the **start** value, while again recording the set number of points. If the light is off, the current is only ramped up. With the option **4-Wire Sense** you can enable the 4-wire (or 4-point) measurement.

After you adjusted all settings, you can load the settings to the instrument (**Load Settings to Instrument**), if you want to check whether everything is set correctly on the instrument. Otherwise, the settings are also loaded to the instrument if you start the measurement. Do this by pressing the **Start Measurement** button. You can then check the current state of the measurement on the SMU's screen. After the measurement is finished, the data is sent to the computer and visualized in the graph of the LabView program. To indicate whether the new measurement data has already

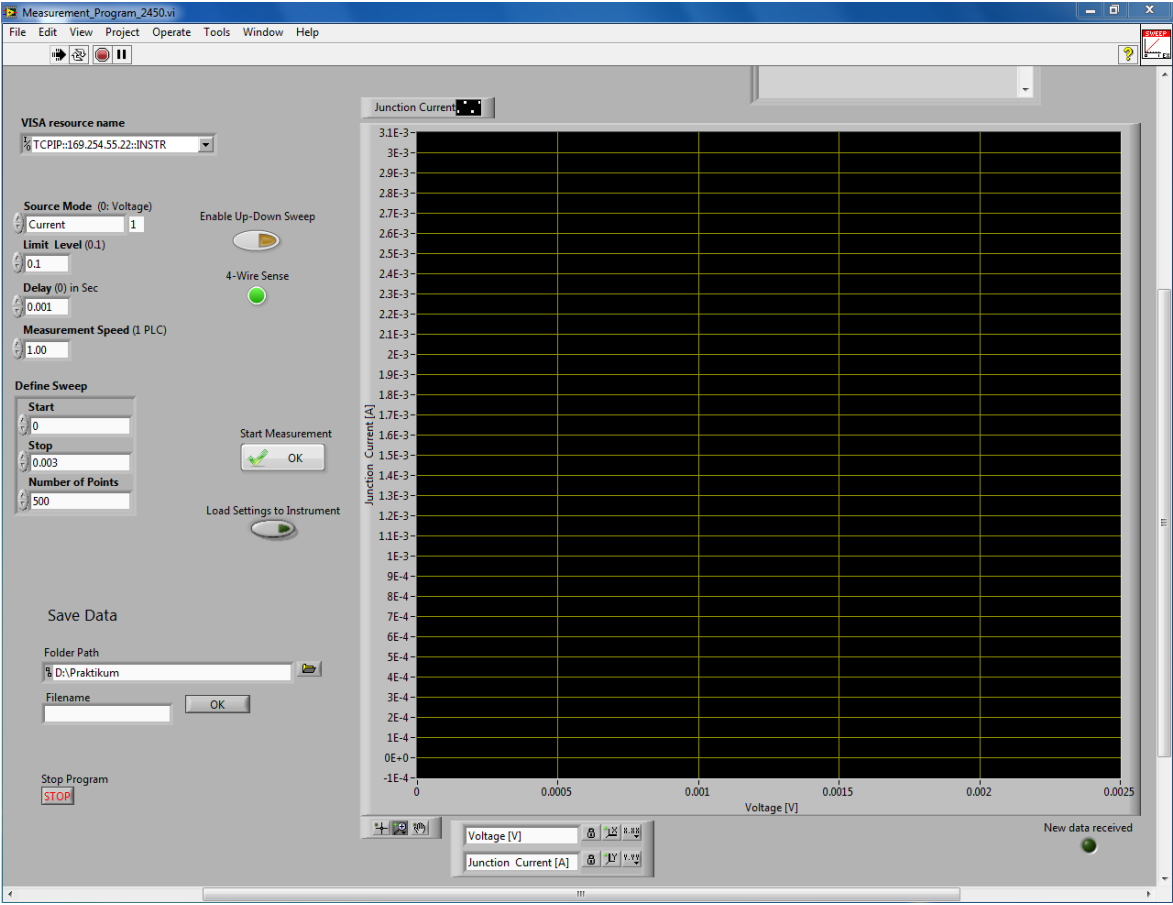


Figure 3.3: Screenshot of the LabView program.

arrived, there is a light in the right bottom corner (**New data received**), which turns off after **Start Measurement** is pressed and turns back on again when the new data has arrived at the computer.

To save the data, create a new folder with your group number in the folder D:\Praktikum\WS1516 (WS1516 should be replaced by the current semester) and write the new folder path in the field **Folder Path**. Afterwards enter the file name for the current measurement and press **OK**. The data of the measurement is now saved in a file, that can be open with standard text editors, such as the windows editor or notepad++, and can also be loaded into data analyzing software, such as Origin.

If the program crashed, you can stop the program with the stop button on the lower left, or the one on the top left and restart it using the run button (arrow in the top left corner).

Chapter 4

Measurement

This section describes in detail the steps you will have to take in order to perform the experiment.

4.1 Cooling down the sample rod

The tutor must attend the mounting of the sample rod on the helium can and the following insertion of it into the liquid helium!

Before you work on the helium can, put on the safety glasses and gloves!

Remove the shutter valve from the He-can and place the sample rod on top of the can. Take care that the sample rod is fixed in its upmost position.

Now slowly lower the sample rod into the He-can until the table tennis ball inside the helium reflow system starts to move. Lower the rod further, until the table tennis ball is in the middle of the tube. Wait until the ball returns to a point well below the middle of the tube and lower the rod further down until the ball rises and wait until it goes down again. Do this until you reach the marker on the rod and wait until the ball has settled, which indicates, that the sample is cold.

4.2 Measuring the I-U-curve

After the sample is cold (see section [4.1](#)), you can start with the measurements. Your first task is to measure a $I - U$ characteristic of the Josephson contact.

1. Make sure, that the source meter is correctly wired to the ports of the connection box. For further information check section [3.3](#).
2. Set the start and stop point of the measurement in LabView to 0 A and 0.003 A. The number of point should be set to 500.

3. In LabView, also enable the **up-down sweep** to be able to check for hysteretic behaviour and enable the **4-wire sense**.
4. Start the measurement by pressing **Start Measurement**.
5. Wait until the **New data received** lamp is on and perform a quick check of the measured data, by comparing it to what you would expect. To get a good feeling for the data, locate the critical current, the ohmic region and check for hysteresis.
6. Save the data as the zero-field measurement.

4.3 Measurement of the field dependent critical current

The second part of the experiment is the measurement of the critical current as a function of an externally applied magnetic field.

1. Make sure that the coil is correctly wired to the connection box and the voltmeter (see section 3.3).
2. Create a measurement plan for the measurement. You should measure the graph shown in figure 2.5 at least up to the second minimum. Calculate what voltage you have to measure at the coil voltmeter in order to create a flux inside the junction which corresponds to the value of the second minimum, which corresponds to $2 \cdot \Phi_0$, with $\Phi_0 = 2.0678 \cdot 10^{-15}$ Wb. Note that 1 V at the voltmeter always corresponds to the maximal value of current set at **I-Range** (see figure 3.2). At a coil current of 200 mA the coil produces a field of 7.95 mT. The flux through the junction can be calculated with $\Phi = A \cdot B$, where B is the magnetic field at the sample and A the area of the junction, which is perpendicular to the field. The area can be calculated as $A = t_B \cdot L$, with the magnetic thickness of the junction $t_B = d + 2\lambda_L = 177.83$ nm and its edge length $L = 19.5$ μ m.
3. Choose an appropriate amount of points you want to measure. You should choose enough points to be able to see the expected shape clearly.
4. Before you start measurements, confirm with the tutor that your measurement plan is sensible.
5. Set the coil current to the first value (**Set I**, fig. 3.2). Measure the I-U characteristic with the LabView program (see section 4.2) and save the data. Repeat this for all measurement points. Consider changing the settings in the Labview program to reduce the required measurement time.

4.4 Warming up the sample rod

The tutor must attend this procedure!

Before you start working on the helium can, put on safety goggles and gloves! Now pull the sample-rod slowly up to the top and wait until it reached room temperature . Next, you can unmount the sample-rod from the helium dewar and remount the shutter valve to the helium dewar. When unmounting the rod, be aware that cold helium gas can be relieved through the gap between the fitting and the sample dip-stick . Make sure you tilt the sample stick slightly towards yourself, thus the helium gas vents away from yourself.

Chapter 5

Exercises

5.1 Questions

Answer the following questions in a written report before doing the experiment. After doing the experiment add the measurement results and conclusions to your report.

1. What are the benefits of a 4-wire (or 4-point) resistance measurement compared to a 2-wire configuration?
2. At which bias voltage do you expect radiation emission of the Josephson-contact with a frequency of 10 GHz? At which bias voltage do you expect the 2nd harmonic to have a frequency of 10 GHz?
3. Derive the 2. Josephson equation (2.10) starting from $i\hbar \frac{\partial}{\partial t} \psi_{1,2} = E_{1,2} \psi_{1,2}$ with respect to the wavefunction of a Cooper-pair, described by Eq. 2.2 ($n = 1$).
4. Derive from equation 2.10 and 2.14 a differential equation for γ . Which analogy exists between the parameters C , R_n , γ , I and the fundamental parameters of a physical pendulum?
5. Show the transformation invariance of equation 2.10.

5.2 Evaluation

5.2.1 Introduction

Present a detailed description of the experimental setup (including the sample) and of the performed measurements. What did you measure? How did you do it?

5.2.2 Zero field measurement

- Determine I_c and I_R .
- Determine R_n .
- Determine the McCumber parameter β_c and thus deduce the damping regime the junction is in ($\beta_c < 1$ or $\beta_c > 1$?). Discuss the impact the regime has on the junction.
- Determine the capacitance of the junction and compare it to a plate capacitor with an area of L^2 , a distance of d and AlO_x as a dielectric.

5.2.3 Field dependent measurements

- Plot and explain the behaviour of I_c with varying flux inside the junction.
- Determine the measured flux quantum Φ_0 , using the periodicity of the behaviour of I_c .
- Fit the data using the formula for the expected behaviour of $I_c(\Phi)$ (see Sec. [2.2.6](#)).
- Discuss possible differences of the determined flux quantum and the literature value.

Bibliography

- [1] Paul H E Meijer. Kamerlingh Onnes and the discovery of superconductivity. American Journal of Physics, 62(12):1105–1108, 1994.
- [2] Rudolf Gross and Achim Marx. Festkörperphysik. Oldenbourg Wissenschaftsverlag, 2nd edition, October 2014.
- [3] J Bardeen, L N Cooper, and J R Schrieffer. Theory of Superconductivity. Phys. Rev., 108:1175, December 1957.
- [4] J Bardeen, L N Cooper, and J R Schrieffer. Microscopic Theory of Superconductivity. Phys. Rev., 106:162, April 1957.
- [5] Leon N Cooper. Bound Electron Pairs in a Degenerate Fermi Gas. Phys. Rev., 104:1189, November 1956.
- [6] H Fröhlich. Phys. Rev. 79, 845 (1950) - Theory of the Superconducting State. I. The Ground State at the Absolute Zero of Temperature. Phys. Rev., 79:845, September 1950.
- [7] H Fröhlich. Interaction of Electrons with Lattice Vibrations. Proceedings of the Royal Society A: Mathematical, Physical and Engineering Sciences, 215(1122):291–298, December 1952.
- [8] F London and H London. The Electromagnetic Equations of the Supraconductor. Proceedings of the Royal Society A: Mathematical, Physical and Engineering Sciences, 149(866):71–88, March 1935.
- [9] A C Rose-Innes and E H Rhoderick. Introduction to Superconductivity, volume 6 of International Series in Solid State Physics. Pergamon Press, New York, 2nd edition, January 1978.
- [10] W Meissner and R Ochsenfeld. Ein neuer Effekt bei Eintritt der Supraleitfähigkeit. Die Naturwissenschaften, 21(44):787–788, November 1933.
- [11] Michael Tinkham. Introduction to Superconductivity. Dover Publications Inc., New York, 2nd edition, June 2004.

- [12] A Barone and G Paterno. Physics and Applications of the Josephson Effect. John Wiley & Sons, Inc., September 1982.